ISSN 1070-3284, Russian Journal of Coordination Chemistry, 2009, Vol. 35, No. 6, pp. 454–459. © Pleiades Publishing, Ltd., 2009.

Synthesis, Crystal Structure and DNA-Binding Studies of the Complex $[Co(C_{10}H_9N_2O_4)_2] \cdot 3H_2O$[1]

Feng Liu[a,b], Wie-Ping Zhang[a], Shui-Yang He[a], and Liu-Jie Wang[a]

[a] *College of Chemistry and Material Science, Northwest University and Key Laboratory of Synthetic and Natural Functional Molecule Chemistry of Ministry Education, Xi'an, Shanxi 710069, P.R. China*

[b] *Quality Management Department Shanxi Heavy Duty Automobile Co, Ltd, Xi'an, Shanxi 7102000, P.R. China*

e-mail: xdchemistry411@126.com

Received October 23, 2008

Abstract—A novel binuclear Cobalt(II) complex with N-(2-propionic acid)-salicyloyl hydrazone ($C_{10}H_{10}N_2O_4$, H_3L) was prepared and characterized. The crystal structure of $[Co(C_{10}H_9N_2O_4)_2] \cdot 3H_2O$ was determined by X-ray single-crystal diffractometry. The Co^{2+} ion is six-coordinated by the carboxyl and acyl O atoms and azomethine N atoms of two tridentate N-(2-propionicacid)-salicyloyl hydrazone ligands, which form two stable five-numbered rings sharing one side in the keto form. The coordination environment around the Co^{2+} ion might be described as a distorted octahedron. Abundant hydrogen bonds of the types O–H···N and O–H···O between the water molecules and ligands not only form the three-dimensional network, but also provide an extrastability for the crystal. The complex was studied for the interaction with calf thymus DNA by electronic absorption titration and emission titration. The results show that the complex is bound to calf thymus DNA mainly by intercalation.

DOI: 10.1134/S1070328409060116

Over the past decade, the DNA-binding metal complexes have been extensively studied as DNA structural probes, DNA footprinting, DNA cleaving agents, potential anticancer drugs, and so on [1–5]. So, the design of small complexes that bind and react at specific sequences of DNA has become quite important. A more complete understanding of how to target DNA sites with specificity will lead not only to novel chemotherapeutics but also to a greatly expanded ability of chemists to probe DNA and to develop highly sensitive diagnostic agents [6].

Transition metal complexes are being used at the forefront of many of these efforts. Stable, inert, and water-soluble complexes containing spectroscopically active metal centers are extremely valuable as probes for biological systems. As both spectroscopic tags and functional models for the active centers of proteins, metal complexes helped to elucidate the mechanisms by which many metalloproteins function [6].

In order to develop new antitumor drugs, which specifically target DNA, it is necessary to understand the different binding modes a metal complex is capable of undergoing. Basically, metal complexes interact with the double helix of DNA in either a noncovalent or a covalent way. The former way includes three binding modes: intercalation, groove binding, and external electrostatic effects. Among these interactions, intercalation is one of the most important DNA binding modes, because it invariably leads to cellular degradation. It was reported that the intercalating ability increases with the planarity of ligands [7, 8]. Additionally, the coordination geometry and ligand donor atom type also play key roles in determining the binding extent of complexes to DNA [9, 10]. The metal ion type and its valence, which are responsible for the geometry of the complexes, also affect the intercalating ability of metal complexes to DNA [11, 12].

A lot of acyl hydrazone complexes have provoked extensive interest because of their diverse spectra of biological and pharmaceutical activities, such as anticancer, antitumor, and antioxidative activities, as well as the inhibition of lipid peroxidation, etc. N-(2-propionic acid)-salicyloyl hydrazone (**H_3L**) constitutes another kind of Schiff bases ligand that has lately been shown to be able to form interesting complexes with lanthanides [13]. Recent results have shown that this type of ligand, when coordinating metal ion may improve biological and pharmaceutical activities of the complexes due to forming special structures with the metal ion. At the same time, there are three coordination forms for the complexes of acyl hydrazone: keto-form, enolic form, and dehydrogenation conjugation form [14–16]. The valence of acyl hydrazone is diverse [17–20]. In this paper, the cobalt(II) complex with the ligand H_3L, $[Co(C_{10}H_9N_2O_4)_2] \cdot 3H_2O$ (**I**), has been synthesized and characterized. Moreover, the Co(II) complex **I** is selected as a target molecule, which is studied

[1] The article is published in the original.

Table 1. Selected bond lengths and bond angles for the complex **I**

Bond	*d*, Å	Bond	*d*, Å
Co(1)–N(4)	2.046(5)	Co(1)–N(2)	2.052(5)
Co(1)–O(3)	2.092(4)	Co(1)–O(7)	2.103(5)
Co(1)–O(2)	2.136(4)	Co(1)–O(6)	2.168(5)
O(1)–C(1)	1.352(7)	O(1)–H(1)	0.8200
O(2)–C(7)	1.254(7)	O(3)–C(9)	1.307(7)
O(4)–C(9)	1.217(8)	O(5)–C(11)	1.360(7)
O(5)–H(5)	0.8200	O(6)–C(17)	1.252(7)
O(7)–C(19)	1.283(7)	O(8)–C(19)	1.248(7)
Angle	ω, deg	Angle	ω, deg
N(4)Co(1)N(2)	173.2(2)	N(4)Co(1)O(3)	97.13(18)
N(2)Co(1)O(3)	76.15(18)	N(4)Co(1)O(7)	75.59(18)
N(2)Co(1)O(7)	104.18(18)	O(3)Co(1)O(7)	96.02(18)
N(4)Co(1)O(2)	111.62(18)	N(2)Co(1)O(2)	75.07(18)
O(3)Co(1)O(2)	151.13(16)	O(7)Co(1)O(2)	88.87(18)
N(4)Co(1)O(6)	74.88(18)	N(2)Co(1)O(6)	105.72(18)
O(3)Co(1)O(6)	92.39(18)	O(7)Co(1)O(6)	150.06(16)
O(2)Co(1)O(6)	97.44(18)		

for the interaction with CT-DNA by electronic absorption titration and emission titration.

EXPERIMENTAL

Calf thymus DNA (**CT-DNA**) was purchased from Sigma (USA). Pyruvic acid was a biochemical reagent. All chemicals used were of analytical grade.

The C, H and N analyses were taken with a Perkin Elmer model 2400 elemental analyzer. The metal ion was determined by titration. Molar conductance measurement was made in DMF using a DDS–11A conductivity meter.

The UV spectra were recorded on a Lambda 40P UV-vis spectrophotometer. Fluorescence measurements were made on a Hitachi F-4500 spectrophotometer.

The interaction of the complex with CT-DNA was studied in a doubly distilled water buffer containing of tris(hydroxymethyl)aminomethane (**Tris**) (5 mmol), 0.4% DMSO, and NaCl (5 mmol). The system was adjusted to pH 7.1 with hydrochloric acid. In order to eliminate the absorbance of nucleic acid itself, an equal amount of CT-DNA was added to the sample and the reference cell, respectively. Spectrometric titrations were performed according to References [21–23].

The X-ray data for the crystal were collected on a Bruker Smart–1000 CCD X-ray single-crystal diffractometer. All the calculations were formed with the SHELXTL–97 program. The water H atoms were located in a difference Fourier map and were refined freely with a distance restraint of O–H 0.86 Å. The H atoms on the C and N atoms were positioned geometrically, with C–H = 0.93 Å for aromatic H, 0.96 Å for methyl H, and N–H 0.86 Å. The final electron density maximum and minimum were 0.757 and –0.594 e/nm^{-3}, respectively. An absorption correction was applied by Multi-scan. Selected bond lengths and bond angles of the crystal are listed in Table 1.

Supplementary material has been deposited with the Cambridge Crystallographic Data Centre (no. 699558; deposit@ccdc.cam.ac.uk or http://www.ccdc. cam.ac.uk).

The synthesis route and physicochemical property of the ligand H_3L was reported in [24].

Synthesis of the complex I. Preporation was performed under hydrothermal conditions. A solution of H_3L (0.224 g, 1 mmol) in 15 ml of aqueous ethanol (1 : 2) was added under stirring to a solution of $CoCl_2 \cdot 6H_2O$ (0.118 g, 0.5 mmol) in 5ml of aqueous ethanol (1 : 2). The pH of the mixture was adjusted to about 6 using triethylamine. The resultant solution was refluxed in 80°C water bath for 2 h and then filtered. The filtrate was left to evaporate naturally for about two weeks at room temperature, and pink prismatic crystals were obtained. The yield is 62%.

For $[Co(C_{10}H_9N_2O_4)_2] \cdot 3H_2O$

anal. calcd, %: Co, 10.61; C, 43.25; H, 4.35; N, 10.09.

Found, %: Co, 10.52; C, 43.41; H, 4.45; N, 10.15.

The Λ_M value (6.5 S cm^2 mol^{-1}) is consistent with the expected value for nonelectrolyte [25]. The complex can be easily dissolved in DMF and DMSO, sparingly soluble in methanol but insoluble in water, ethanol, and benzene.

RESULTS AND DISCUSSION

The X-ray single-crystal analysis revealed that the complex consists of a neutral $[Co(C_{10}H_9N_2O_4)_2]$ unit and three free water molecules. The Co^{2+} ion is six-coordinated by linking two tridentate ligands H_3L through the acyl oxygen, carboxyl oxygen and imido nitrogen (Figs. 1a, 1b). Thus, two five-membered chelate rings sharing one edge are formed for each ligand. At the same time, the atoms O(6), N(2), O(7), and N(4) are coplanar approximately and form the equatorial plane. While two oxygen atoms of another ligand occupy the axial sites, the angle of the axial O(5)Co(1)O(7) is 150.09°, which deviates from the linear angle of 180°. These data indicate that the Co(1)

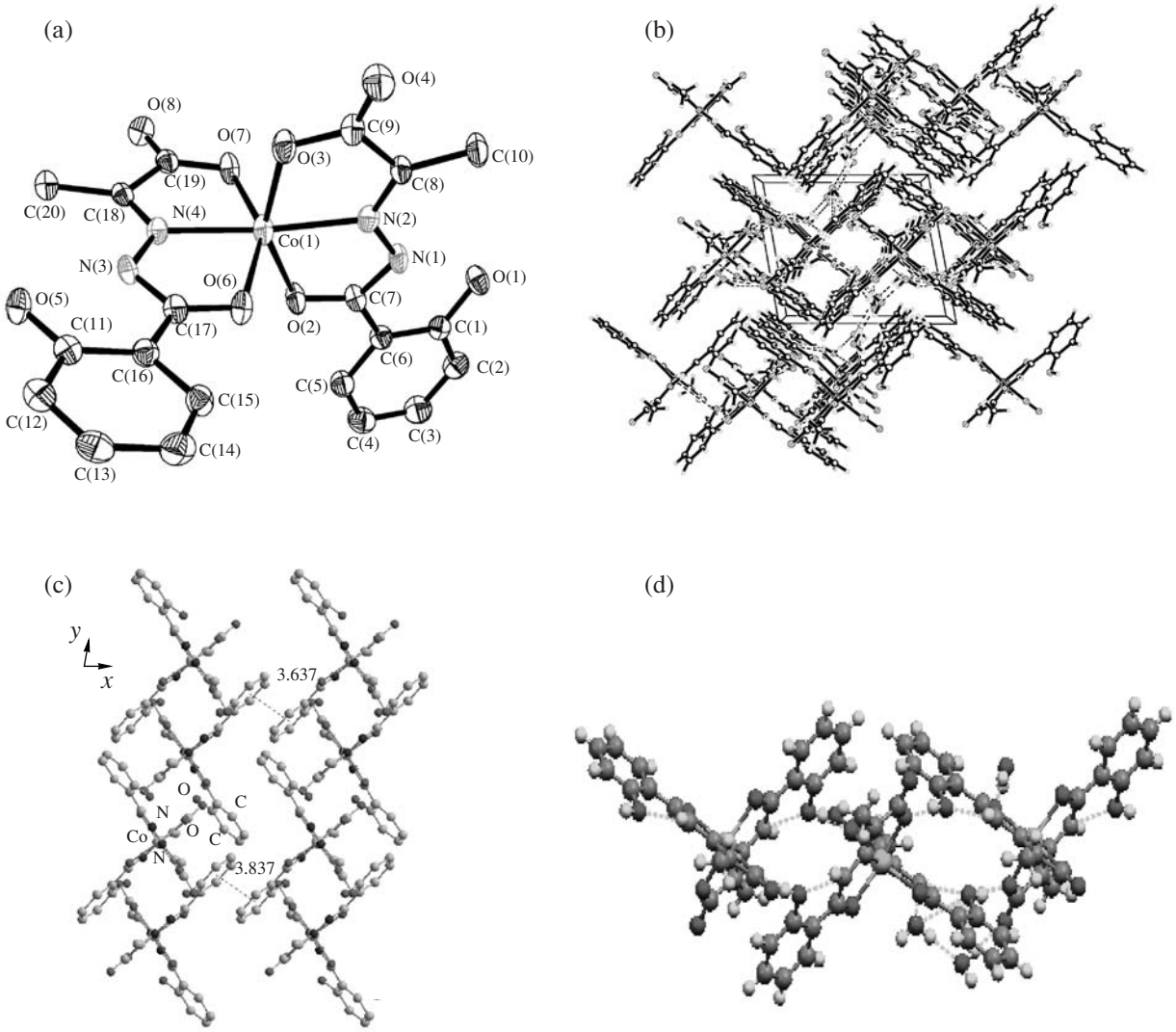

Fig. 1. Perspective view of coordination for the complex **I** (a), packing diagram (b) (H atoms are omitted for clarity), π–π stacking (c), tripolymer (d).

atom is in the distorted octahedron geometry. Noncoordinated three water molecules are found in the crystal lattice. From the perspective of the complex, the atoms of each H_3L are almost located on the same plane in Fig. 1, and the angle of the two planes is 83.95°. Comparing with the distances of C–O (1.42 Å) and C = O (1.23 Å), the bond lengths of O(6)–C(17) and O(2)–C(7) are 1.252 and 1.253 Å, respectively, indicating that these bonds are single bond and the ligand functions as a keto form.

There are abundant hydrogen bonds in the molecule (Table 2). The intramolecular hydrogen bonds were formed by the nitrogen atom and oxygen atom of the ligand, such as N(1)–H···O(1) and N(3)–H···O(5). At the same time, the intermolecular hydrogen bonds exist between free waters and ligands. Moreover, there are π–π stacking between one benzene ring of the ligand and another benzene ring in the complex, and the distance between each other is 3.637Å (Fig. 1c). It belongs to the medium-strength π–π interaction. These hydrogen bonds and π–π stacking not only make the crystal formed by the three dimensional network but also provide an extrastability for the crystal. In addition, the tripolymer of the complex forming by hydrogen bonds resembles a flying Boeing plane (Fig. 1d).

Before reacting of the Co(II) complex with CT-DNA, its solution behavior in a buffer solution at room temperature was monitored by UV-vis spectroscopy for 24 h. No liberation of the ligand was observed under these conditions. These data suggest that the complex is stable under the conditions studied.

The absorption spectra of the Co(II) complex in the absence and presence of DNA are shown in Fig. 2. With increasing DNA concentrations, the absorption bands at 292 nm for the Co(II) complex exhibit hypochromism of 40%. The hypochromism observed for the

Table 2. Hydrogen bonds in the complex **I***

Contact D–H···Å	*d*, Å			Angle DHA, deg
	D–H	H···A	D···A	
O(1)–H(1)···O(7)$^{\#1}$	0.82	1.84	2.646(6)	168
O(5–H(5)···O(3)$^{\#2}$	0.82	1.74	2.557(6)	171
O(9)–H(1W)···O(8)$^{\#3}$	0.85	2.06	2.909(11)	179
O(9)–H(2W)···O(2)	0.85	2.14	2.994(11)	179
O(10)–H(3W)···O(9)$^{\#4}$	0.85	1.75	2.604(14)	180
O(10)–H(4W)···O(8)	0.85	1.98	2.834(7)	180
O(11)–H(5W)···O(10)	0.85	1.93	2.776(8)	179
O(11)–H(6W)···O(4)$^{\#5}$	0.82	2.19	2.888(7)	143
N(1)–H(1D)···O(1)	0.86	2.07	2.650(6)	125
N(1)–H(1D)···O(11)$^{\#1}$	0.86	2.21	2.867(7)	133
N(3)–H(3D)···O(5)	0.86	1.93	2.579(6)	131

* The symmetric transformations used to generate equivalent atoms: $^{\#1}$ $-x+1, -y+1, -z+1$; $^{\#2}$ $-x+1, -y+2, -z+2$; $^{\#3}$ $-x+1, -y+1, -z+2$; $^{\#4}$ $x-1, y, z$; $^{\#5}$ $x, y-1, z$.

$\pi \longrightarrow \pi^*$ transition bands of the Co(II) complex at 292 nm are accompanied by more than 1 nm red-shift. After the Co(II) complex binds to the base pairs of DNA, the π^* orbit of the intercalated ligand could couple with π orbit of the base pairs, thus, decreasing the $\pi \longrightarrow \pi^*$ transition energies. On the other hand, the coupled π^* orbit is partially filled by electrons, thus, decreasing the transition probabilities. Thus, these effects result in the hypochromism [26]. Large hypochromism of an aromatic dye in the presence of double helical DNA is usually characteristic of intercalation into DNA base pairs for the dye, due to the strong stacking interaction between the aromatic chromophore and the base pairs [27, 28]. So, the above phenomena imply that the complex interacts with calf thymus DNA quite probably by intercalating the ligand into the base pairs.

The Co(II) complex can emit strong luminescence in a Tris buffer with a maximum wavelength of about 411.5 nm. The emission spectra of Co(II) complex in the absence and presence of DNA are illustrated in Fig. 3. It is evident that the emission intensity increases and grows to about 1.2 times with increasing concentrations of CT-DNA for the Co(II) complex. The results of the emission titrations also indicate that the complex is protected from solvent water molecules by the hydrophobic environment inside the DNA helix. This implies that the complex can insert between the DNA base pairs. Since the hydrophobic environment inside the DNA helix reduces the accessibility of the solvent water molecules into the complex, the compound is restricted at the binding site, decreasing the vibrational modes. The binding of the Co(II) complex to DNA

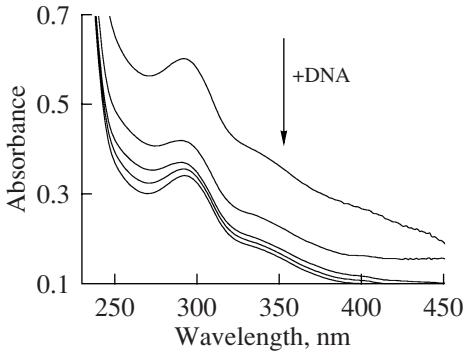

Fig. 2. Electronic spectra of the Co(II) complex (1.0×10^{-4} mol/l) in the presence of CT-DNA. [DNA] = 0, 10×10^{-6}, 20×10^{-6}, 30×10^{-6}, and 40×10^{-6} mol/l.

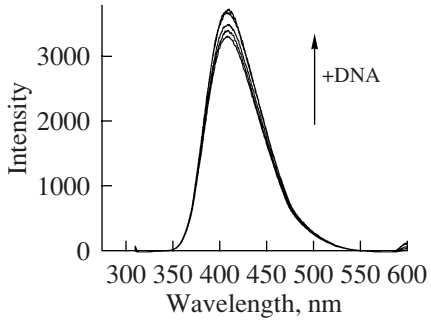

Fig. 3. The emission enhancement spectra of the complex **I** (1.0×10^{-4} mol/l) in the presence of 0.10×10^{-6}, 20×10^{-6}, and 30×10^{-6} mol/l CT-DNA.

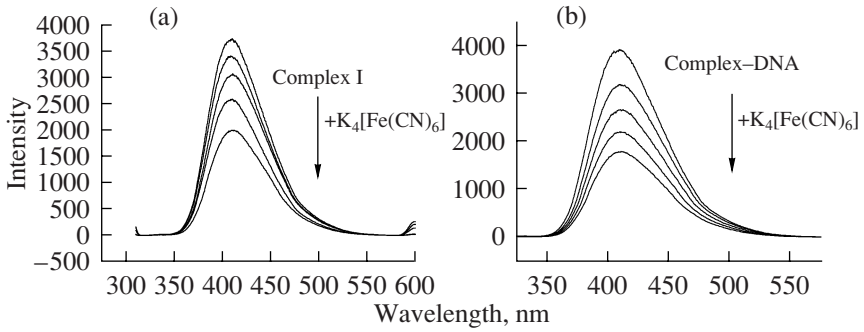

Fig. 4. Emission quenching spectra of complex **I** (a) and complex-DNA (b) with increasing of concentration of the $K_4[Fe(CN)_6]$ quencher. $c_I = 1.0 \times 10^{-4}$ mol/l; $c_{K_4[Fe(CN)_6]} = 0$, 0.5, 1, 1.5, and 2×10^{-3} mol/l, and $c_{DNA} = 40 \times 10^{-6}$ mol/l.

leads to a marked increase in the emission intensity, which also agrees with those observed for the UV spectra.

The emission quenching spectra of the complex **I** in the absence and presence of DNA are shown in Fig. 4. With increasing of the $K_4[Fe(CN)_6]$ quencher concentrations, the system of the complex and complex-DNA causes obvious reduction in emission intensity, but the emission intensity of the complex in the absence of DNA are less than that in the presence of DNA under the same concentration of the $K_4[Fe(CN)_6]$ quencher, indicating that the Co(II) complex binds to DNA and is protected from the $K_4[Fe(CN)_6]$ quencher in the presence of DNA. In addition, it is evident that the emission quenching curvilinear slope in the absence of DNA is larger than that in the presence of DNA (Fig. 5). Furthermore, the emission quenching curve is still close to a beeline after bonding to DNA, which suggests that there is only a bonding mode between the complex and DNA. That is, the Co(II) complex possibly is bound to calf thymus DNA mainly by intercalation.

For further research, the interaction of Co(II) complex with DNA, the steady-state emission quenching experiment was given. Competitive binding to DNA of the free Co(II) complex with ethidium bromide (**EB**) could provide a rich information regarding the DNA-binding nature and relative DNA-binding affinity [29]. Due to strong intercalation between the adjacent DNA base pairs, EB emits intense fluorescence in the presence of DNA. It was previously reported that the enhanced fluorescence could be quenched, at least partially, by the addition of the second intercalative molecule. The quenching extent of fluorescence for EB bound to DNA is used to determine the relative DNA-binding affinity of the second molecule [30]. The emission band at 588 nm of the DNA–EB system decreased in intensity with an increase in the concentration of the compounds, indicating that the compounds could displace EB from the DNA–EB system. Figure 6 displays a well-behaved emission spectrum of EB bound to DNA in the absence and presence of the Co(II) complex.

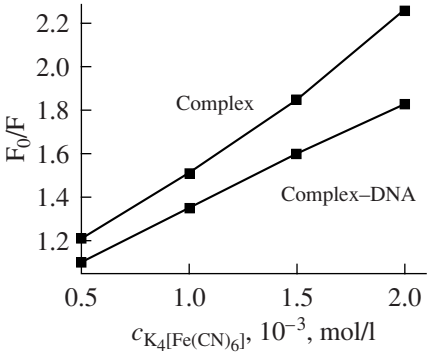

Fig. 5. Emission quenching curve of the complex **I** with increasing of concentration of $K_4[Fe(CN)_6]$ quencher. F_0 and F is the fluorescence intensity of complex **I** in the of absence and in the presence of DNA, respectively.

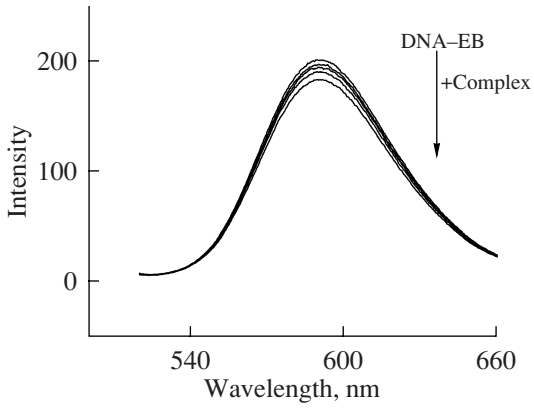

Fig. 6. Emission spectra of the DNA–EB system(10 and 0.32 μM EB), λ_{ex} = 500 nm, λ_{em} = 520.0–660.0 nm, in the presence of 0, 0.5, 1, 1.5, 2, and 2.5×10^{-4} mol/l Co(II) complex.

ACKNOWLEDGMENTS

The work was supported by the program of technological plan of Shanxi Province (no. 2007K02-11).

REFERENCES

1. Wu, B.Y., Gao, L.H., Duan, Z.M., and Wang, K.Z., *J. Inorg. Biochem.*, 2005, vol. 99, p. 1685.
2. Erkkila, K.E., Odom, D.T., and Barton, J.K., *Chem. Rev.*, 1999, vol. 99, p. 2777.
3. Metcalfe, C. and Thomas, J.A., *Chem. Soc. Rev.*, 2003, vol. 32, p. 215.
4. Haq, I., Lincoln, P., Suh, D., et al., *J. Am. Chem. Soc.*, 1995, vol. 117, p. 4788.
5. Arturo, S., Giampaolo, B., Giuseppe, R., et al., *J. Inorg. Biochem.*, 2004, vol. 98, p. 589.
6. Erkkila, K.E., Odom, D.T., and Barton, J.K., *Chem. Rev.*, 1999, vol. 99, p. 2777.
7. Kumar, C.V., Barton, J.K., and Turro, N.J., *J. Am. Chem. Soc.*, 1985, vol. 107, p. 5518.
8. Xu, H., Zheng, K.C., Chen, Y., et al., *Dalton Trans.*, 2003, vol. 11, p. 2260.
9. Mahadvan, S. and Palaniandavar, M., *Inorg. Chim. Acta*, 1997, vol. 254, p. 291.
10. Xu, H., Zheng, K.C., Deng, H., et al., *New J. Chem.*, 2003, vol. 27, no. 8, p. 1255.
11. Asadi, M., Safaei, E., Ranjbar, B., and Hasani, L., *New J. Chem.*, 2004, vol. 28, no. 10, p. 1227.
12. Chaires, J.B., *Biopolymers*, 1998, vol. 44, p. 201.
13. Chen, F.Y., Cao, W.K., Liu, X.R., et al., *Synth. React. Inorg. Met-Org. Nano-Met. Chem.*, 2006, vol. 36, p. 569.
14. Paschalidis, D.G., Tossidis, I.A., and Gdaniec, M., *Polyhedron*, 2000, vol. 19, p. 2629.
15. Yang, Z.Y., Yang, R.D., Li, F.S., et al., *Polyhedron*, 2000, vol. 19, p. 2599.
16. Deng, R.W., Wu, J.G., and Chen, Z.N., *Synth. React. Met.-Org. Chem.*, 1992, vol. 22, p. 1295.
17. Singh, P.K. and Singh, B., *Indian J. Chem., Sect. A: Inorg., Bio-inorg., Phys., Theor. Anal. Chem.*, 1998, vol. 37, p. 331.
18. Shen, X., Xie, Y.Y., and Jiang, H.L., *Synth. React. Inorg. Met.-Org. Chem.*, 1995, vol. 25, p. 511.
19. Wang, M.X., Den, H.Q., and Shan, W.D., *Chin. Chem. Lett.*, 1991, vol. 2, p. 587.
20. He, S.Y., Liu, Y., Zhao, J.S., et al., *Chin. J. Chem.*, 2003, vol. 21, p. 139.
21. Satyanarayana, S., Dabrowiak, J.C., and Chaires, J.B., *Biochemistry*, 1992, vol. 31, p. 9319.
22. Wang, Y. and Yang, Z.Y., *Transition Met. Chem.*, 2005, vol. 30, p. 902.
23. Li, H.B., Wang, X.P., Liu, H.P., et al., *Chin. J. Inorg. Chem.*, 2006, vol. 22, p. 9.
24. He, S.Y., Liu, Y., Zhao, J.S., et al., *Chin. J. Chem.*, 2003, vol. 21, p. 2.
25. Geary, W.J., *Coord. Chem. Rev.*, 1971, vol. 7, p. 81.
26. Hecht, S.M. and Nat, J., *J. Nat. Prod.*, 2000, vol. 63, no. 1, p. 158.
27. Bloomfield, V.A., Crothers, D.M., and Tinico, I.J., *Physical Chemistry of Nucleic Acids,* New York: Harper and Row, 1974, p. 187.
28. Wilson, W.D., Ratmeyer, L., Zhao, M., et al., *Biochemistry*, 1993, vol. 32, p. 4098.
29. Li, H., Le, X.Y., Pang, D.W., et al., *J. Inorg. Biochem.*, 2005, vol. 99, p. 2240.
30. Kumar, C.V., Barton, J.K., and Turro, M.J., *J. Am. Chem. Soc.*, 1985, vol. 107, p. 5518.